



OPEN

## Laryngeal and pleural ultrasound and acoustic radiation force impulse elastography in dogs with brachycephalic obstructive airway syndrome

Ariadne Rein<sup>1</sup>, Andréia Coutinho Facin<sup>1</sup>, Isabella de Almeida Fabris<sup>1</sup>, Bruna Bressianini Lima<sup>1</sup>, Beatriz Gasser<sup>2</sup>, Luiz Paulo Nogueira Aires<sup>1</sup>, Ricardo Andres Ramirez Uscategui<sup>3</sup>, Marcus Antônio Rossi Feliciano<sup>4</sup>✉ & Paola Castro Moraes<sup>1</sup>

This study aimed to evaluate the pleural thickness, stiffness, and laryngeal stiffness in dogs clinically affected by brachycephalic obstructive airway syndrome using B-mode ultrasound and acoustic radiation force impulse elastography. Fifty-two brachycephalic pugs and French bulldogs, clinically classified as having brachycephalic obstructive airway syndrome (BOAS) grades 0, I, II, and III, were included, and 15 mesocephalic beagle dogs were used as the control group (CO). All animals underwent B-mode ultrasonography and subsequent elastography of the pleura and arytenoid cartilage of the larynx. Brachycephalic dogs showed greater pleural thickness than the control group dogs ( $p=0.008$ ) and a trend toward lower pleural shear wave velocity was observed in brachycephalic dogs compared to CO ( $p=0.18$ ). The larynx shear wave velocity was similar between types of skull and BOAS grades ( $p=0.80$ ). Measurements of the pleural line thickness and pleural stiffness showed moderate capacity for diagnosing brachycephalic syndrome ( $p=0.01$ , cut-off value of  $> 0.82$  mm and  $p=0.04$ , cutoff value 3.29 m/s). The results suggest a secondary change in inspiratory effort at the tissue level of the pleura in dogs clinically affected by BOAS, which can be identified by B-mode ultrasound and elastography methods; however, it was not possible to diagnose changes in the arytenoid cartilage.

**Keywords** Arytenoid, French bulldog, Hypoxia, Respiratory obstruction, Pleural thickness, Shear wave velocity

Brachycephalic obstructive airway syndrome (BOAS) in dogs is characterized by a combination of anatomical abnormalities that lead to upper respiratory tract obstruction<sup>1</sup>. An exponential increase has been reported in the demand for brachycephalic dog breeds among pet owners. This growing popularity raises ethical concerns about the welfare of these animals, particularly regarding the conformational health issues that they can develop<sup>2</sup>. Although several affected dogs appear clinically normal, they often experience chronic hypoxia and systemic consequences<sup>3</sup>.

BOAS has a complex pathogenesis and studies have suggested similarities to human obstructive sleep apnea syndrome (OSA), a highly prevalent condition<sup>4</sup>. Patients with OSA have a high prevalence of idiopathic pulmonary fibrosis and other interstitial lung diseases, likely due to increased upper airway resistance, which affects the lower respiratory tract and lung parenchyma<sup>5</sup>. However, studies examining the impact of BOAS on the respiratory system of dogs are limited, and the long-term consequences of this syndrome are not fully understood.

In this context, ultrasound is a portable, cost-effective imaging modality that allows examinations with acceptable reliability and has been recognized as an important diagnostic and prognostic tool for lesions in both the upper and lower respiratory tracts in humans<sup>6,7</sup>. B-mode ultrasound has been specifically used to diagnose

<sup>1</sup>School of Agricultural and Veterinary Sciences, Department of Veterinary Clinic and Surgery, FCAV UNESP, Jaboticabal, SP, Brazil. <sup>2</sup>Institute of Agricultural Sciences, Federal University of the Jequitinhonha and Mucuri Valleys, Unaí, Minas Gerais, Brazil. <sup>3</sup>Universidad del Tolima, Tolima, Colombia. <sup>4</sup>Department of Veterinary Medicine, University of São Paulo e FZEA - USP, Pirassununga, São Paulo, Brazil. ✉email: marcusfeliciano@usp.br

infantile laryngomalacia, obtain anatomical and clinical parameters of the upper airways in adults<sup>9–11</sup> and has been applied to evaluate disorders of the cranial respiratory tract in dogs.

Elastography is a specialized ultrasound modality that has been studied extensively over the past decade. This technique measures tissue stiffness by means of an automated method known as acoustic radiation force impulse (ARFI), is non-invasive, safe, and has proven accuracy for diagnosing various conditions<sup>12,13</sup>. Pulmonary elastography has shown promising results in the diagnosis and monitoring of a range of pulmonary diseases in humans<sup>6,14</sup>. Despite their potential, there is limited information on the application of these techniques in both humans and animals for the identification of the consequences of OSA or BOAS.

Taking these precepts into account, the aim of this study was to evaluate pleural B-mode ultrasound, pleural elastography, and laryngeal elastography to investigate the consequences of BOAS on the cranial and caudal respiratory tracts of affected dogs.

## Results

Among the 52 brachycephalic dogs evaluated, 30 (57.7%) were female and 22 (42.3%) were male. The most frequent breed was the French Bulldog (34, 65.4%), followed by pugs (18, 34.6%). The control group included 15 mesocephalic beagles, of which 11 (73.3%) were female and 4 (26.6%) were male.

The functional classification of the BOAS in brachycephalic dogs was determined using the criteria described by Riggs et al.<sup>38</sup>. Based on this classification system, 14 dogs were classified as grade 0 (26.9%), 15 as Grade I (28.8%), 11 as Grade II (21.15%), and 12 as Grade III (23%). The mean age was significantly lower in brachycephalic dogs classified as grade 0 ( $p=0.003$ ) than in those with other BOAS grades and control group (CO). Similarly, the body condition score (BCS) was significantly lower in dogs classified as Grades 0 and I ( $p=0.026$ ) than in those classified as Grades II and III. The primary clinical characteristics of the animals are shown in Table 1.

None of the 67 evaluated dogs exhibited relevant radiographic abnormalities. On B-mode chest ultrasound examination, all animals demonstrated the presence of A-lines, the seashore sign, normal pleural sliding, and no echogenicity changes. Only one brachycephalic dog, a 5-year-old pug clinically classified as BOAS Grade I, showed moderate B-lines without significant radiographic abnormalities or clinical symptoms.

Brachycephalic dogs had significantly greater pleural thickness than the controls ( $p=0.008$ ). Furthermore, dogs classified as BOAS Grades II and III exhibited greater pleural thickness than those classified as grade 0 or I ( $p=0.008$ ).

Although there was a numerical trend toward lower SWV values in the brachycephalic group, the pleural shear wave velocity (SWV) measurements, assessed using quantitative elastography, were similar between brachycephalic and CO ( $p=0.181$ ). Depth measurements of pleural SWV were significantly greater in brachycephalic dogs, particularly in those classified as BOAS Grades II and III ( $p<0.001$ ) (Fig. 1).

The laryngeal SWV was similar between brachycephalic and CO and across BOAS grades ( $p=0.805$ ). The depth of laryngeal SWV measurements was greater in brachycephalic dogs than in the CO ( $p<0.001$ ); however, no significant differences were noted between the BOAS grades ( $p=0.352$ ) (Table 2, Fig. 2).

Receiver operating characteristic (ROC) curve analysis was performed to evaluate the diagnostic accuracy of pleural line thickness, pleural SWV, and laryngeal SWV in identifying brachycephalic syndromes. Pleural line thickness and pleural SWV demonstrated moderate diagnostic accuracy ( $p=0.001$ , cutoff  $>0.82$  mm, sensitivity = 42%, specificity = 90%; and  $p=0.04$ , cutoff  $<3.29$  m/s, sensitivity = 42%, specificity = 90%,

Variable	Group	Mean	SD	p value
Age (years)	G0 <sup>B</sup>	1.8	1.4	0.003
	G1 <sup>A</sup>	3.4	1.6	
	G2 <sup>A</sup>	3.5	1.7	
	G3 <sup>A</sup>	4.1	1.7	
	CO <sup>A</sup>	3.6	1.2	
Weight (kg)	G0	11.1	2.9	0.395
	G1	10.9	2.6	
	G2	11.9	2.7	
	G3	12.4	3.3	
	CO	10.7	1.4	
BCS	G0A <sup>B</sup>	5.9	0.9	0.026
	G1 <sup>B</sup>	5.4	1.0	
	G2 <sup>A</sup>	6.4	0.6	
	G3 <sup>A</sup>	6.4	1.1	
	CO <sup>AB</sup>	5.9	0.5	

**Table 1.** Mean  $\pm$  SD and statistical results (ANOVA) for age (years), body condition score (BCS), and weight (kg) in 52 brachycephalic dogs and 15 mesocephalic dogs. The mesocephalic group is represented as the control group (CO), while brachycephalic dogs are clinically classified as BOAS G0 (grade 0), G1 (grade I), GII (grade II), and GIII (grade III). \*Groups followed by the same letters indicate no statistically significant difference (Tukey post-hoc test).

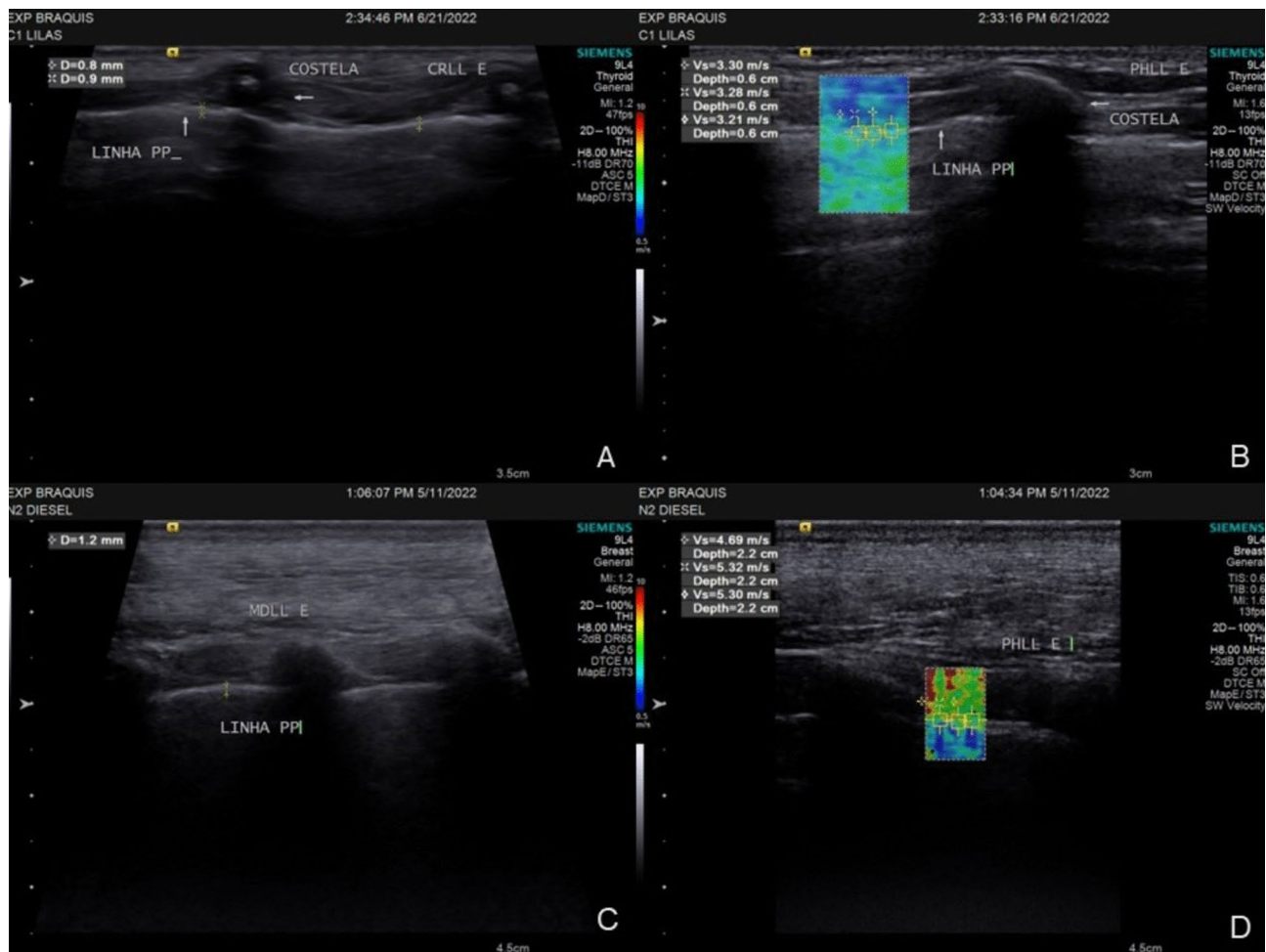


**Fig. 1.** B-mode ultrasound and ARFI elastography of the pleural line. (A) and (B) mesocephalic dog from the control group. (A) B-mode ultrasound image showing the pleural line (linha PP). (B) ARFI elastography of the pleural line in the same individual as (A), demonstrating the region of interest for shear wave velocity (SWV) analysis. (C) and (D) dog classified as BOAS Grade III, highlighting potential pleural abnormalities. (C) B-mode ultrasound image of the pleural line (linha PP). (D) ARFI elastography of the pleural line in the same dog as in (C), illustrating SWV measurements and changes in pleural elasticity.

respectively). However, laryngeal SWV did not show a diagnostic accuracy for brachycephalic syndrome ( $p=0.598$ ). The results are summarized in Table 3.

Correlation analysis revealed no significant relationship between age and the primary variables. Body weight showed a strong positive correlation with laryngeal SWV, and a moderate positive correlation with the pleural line thickness, pleural depth, and laryngeal depth. Additionally, BCS showed a moderate positive correlation with the pleural depth, laryngeal SWV, and laryngeal depth. The pleural line thickness was moderately correlated with both pleural and laryngeal depths, whereas laryngeal SWV showed a moderate positive correlation with laryngeal depth. A detailed correlation analysis of age, body weight, BCS, and the objective measures is presented in Table 4.

## Discussion

Our study identified an increased pleural thickness in brachycephalic dogs clinically affected by BOAS, particularly in those classified as grade II and III. Additionally, there was a trend toward lower pleural stiffness in these dogs, suggesting tissue-level alterations secondary to upper airway obstruction. No changes in arytenoid cartilage stiffness were detected using ARFI elastography, which may reflect technical challenges rather than the absence of secondary laryngeal alterations. These findings highlight the potential consequences of BOAS on the respiratory system and the utility of imaging methods, such as ultrasound, in the diagnosis and monitoring of the clinical evolution of the syndrome.

B-mode ultrasound revealed normal lung characteristics<sup>15</sup>, including horizontal A-lines, lung sliding, and pleural movement, in most evaluated dogs, regardless of brachycephaly. However, one BOAS Grade I dog exhibited B-lines without accompanying clinical or radiographic changes. B-lines, previously termed comet tail artifacts are hyperechoic reverberations associated with edematous interlobular septa and visceral pleura. While

Variable	BOAS grades	Median	IQR	p value
Pleural line thickness	CO <sup>A</sup>	0.70	0.10	0.008
	G0 <sup>B</sup>	0.75	0.13	
	G1 <sup>B</sup>	0.75	0.15	
	G2 <sup>C</sup>	0.85	0.15	
	G3 <sup>C</sup>	0.80	0.34	
Pleural SWV	CO	4.02	0.72	0.181
	G0	3.87	1.24	
	G1	3.71	0.98	
	G2	3.84	1.26	
	G3	3.79	0.82	
Pleural depth	CO <sup>A</sup>	0.92	0.32	0.000
	G0 <sup>B</sup>	1.38	0.49	
	G1 <sup>B</sup>	1.23	0.50	
	G2 <sup>C</sup>	1.45	0.25	
	G3 <sup>C</sup>	1.43	0.68	
Laryngeal SWV	CO	7.14	1.08	0.805
	G0	7.38	2.07	
	G1	7.63	2.27	
	G2	7.67	2.64	
	G3	7.78	3.25	
Laryngeal depth	CO <sup>A</sup>	0.92	0.28	0.000
	G0 <sup>B</sup>	1.38	0.49	
	G1 <sup>B</sup>	1.23	0.50	
	G2 <sup>B</sup>	1.45	0.25	
	G3 <sup>B</sup>	1.43	0.68	

**Table 2.** Median  $\pm$  interquartile range of pleural line thickness measured by B-mode ultrasound, pleural shear wave velocity (SWV, m/s) obtained by Acoustic Radiation Force Impulse (ARFI) elastography, and the depth of this examination; laryngeal SWV and the depth of this evaluation. Data were collected from 52 brachycephalic dogs clinically classified as BOAS G0 (grade 0), G1 (grade I), GII (grade II), and GIII (grade III), and 15 mesocephalic dogs (CO: Control group). \*Groups followed by the same letters indicate no statistically significant difference (Dunns post-hoc test).

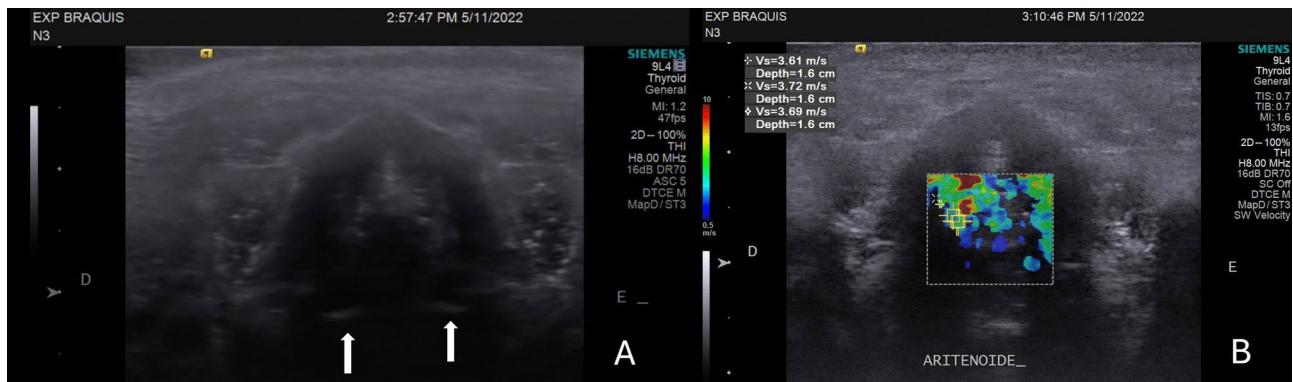


**Fig. 2.** B-mode ultrasound and ARFI elastography of the larynx in a dog from the brachycephalic group. (A) B-mode ultrasound image of the larynx showing the cuneiform process of the arytenoid cartilage (white arrows). (B) ARFI elastography of the larynx, illustrating the region of interest (ROI) for shear wave velocity (SWV) analysis and cartilage elasticity evaluation.

B-lines are typically linked to cardiopulmonary edema, acute respiratory distress syndrome, or pulmonary fibrosis in dogs<sup>16</sup>, their presence in this asymptomatic animal is likely incidental.

The pleural line, defined as a hyperechoic horizontal structure separating the chest wall and lung, can exhibit alterations in thickness due to underlying pathology, increased pleural thickness is associated with subpleural fibrotic lesions in both animals and humans<sup>14</sup>. In neonates, “thick”, “irregular”, or “coarse” pleural lines have

Variables	Parameters	BOAS diagnostic
Pleural Line thickness (mm)	<i>p</i> value	0.0146
	Cut-off value	> 0.825
	Sensitivity %	42.11
	Specificity %	89.66
Pleural SWV (m/s)	<i>p</i> value	0.0416
	Cut-off value	< 3.293
	Sensitivity %	36.84
	Specificity %	89.66
Laryngeal SWV (m/s)	<i>p</i> value	0.5988
	Cut-off value	> 7.575
	Sensitivity %	N/A
	Specificity %	N/A

**Table 3.** Diagnostic performance variables (ROC curve analysis) of Pleural line thickness (mm), Pleural SWV (shear wave velocity of pleural line in m/s), and Laryngeal SWV (sear wave velocity of larynx in (m/s), for diagnosis of brachycephaly obstructive airway syndrome (BOAS Grade I-III). N/A indicates that diagnostic accuracy was not available due to insufficient data or lack of predictive value.

Variable	Statistics	Age	Weight	BCS	Pleural line thickness	Pleural SWV	Laryngeal SWV
Pleural line thickness (mm)	r-Spearman	0.140	0.327	0.232	N/A	N/A	N/A
	<i>p</i> value	0.261	0.007	0.059	N/A	N/A	N/A
Pleural SWV (m/s)	r-Spearman	0.130	-0.060	0.06	0.040	N/A	N/A
	<i>p</i> value	0.286	0.590	0.620	0.690	N/A	N/A
Pleural depth (cm)	r-Spearman	0.043	0.460	0.550	0.490	-0.223	N/A
	<i>p</i> value	0.734	0.001	0.001	0.001	0.070	N/A
Laryngeal SWV (m/s)	r-Spearman	0.161	0.960	0.420	0.330	0.170	N/A
	<i>p</i> value	0.198	0.001	0.001	0.060	0.168	N/A
Laryngeal depth (cm)	r-Spearman	0.043	0.470	0.550	0.490	-0.224	0.399
	<i>p</i> value	0.734	0.001	0.001	0.001	0.069	0.001

**Table 4.** Results of Spearman's correlation analysis between pleural line thickness, pleural and laryngeal shear wave velocity (SWV), depth of these evaluations, and demographic variables such as age, weight, and body condition score (BCS). N/A indicates that correlation was not available.

been correlated with respiratory distress syndrome and pneumonia, though this assessment remains operator dependent<sup>17</sup>. In our study, brachycephalic dogs exhibited greater pleural thickness compared to controls, with the most pronounced alterations in BOAS Grades II and III. This finding suggests that dynamic respiratory obstruction in brachycephalic dogs contributes to airway resistance, edema, and subsequent pleural alterations. This vicious cycle likely exacerbates respiratory distress in BOAS-affected dogs, as previously described in the previous literature<sup>17,18</sup>.

Diagnostic imaging methods such as ultrasound and computed tomography are crucial for characterizing pleural pathology and guiding management. Pleural thickening is associated with various inflammatory, infectious, and neoplastic processes<sup>19</sup>. Using a 9-MHz linear transducer in this study provided high accuracy for detecting pleural changes owing to its suitability for evaluating superficial tissues<sup>20,21</sup>. Chronic respiratory obstruction in BOAS-affected dogs may explain the increased pleural thickness observed in more advanced grades, which is consistent with findings in elderly animals and humans<sup>20</sup>.

ARFI elastography, which quantitatively assesses the tissue elasticity, has shown diagnostic utility for various canine organs, including the liver, spleen, and kidney<sup>22</sup>. Facin et al.<sup>23</sup> noted increased liver and spleen stiffness in brachycephalic dogs with BOAS compared with that in mesocephalic controls. Despite its limitations in lung imaging owing to the reflection of ultrasound waves by air-filled alveoli, elastography is gaining interest for evaluating respiratory diseases in humans<sup>6</sup>. Since BOAS in dogs is considered analogous to OSA in humans, interstitial lung disease, characterized by fibrosis and stiffness, is expected in affected individuals.

Contrary to our hypothesis, pleural stiffness in brachycephalic dogs did not differ significantly from that in controls, although there was a downward trend in SWV. Factors such as young age (mean: 3.2 years) and adequate BCS (mean: 6.1) may explain the absence of significant differences, as older age, chronicity, and obesity are associated with greater stiffness in OSA<sup>4,24,25</sup>. Instead, the observed trend toward lower pleural stiffness may indicate inflammation, as elastography studies in human inflammatory diseases (e.g., Crohn's disease, glomerulonephritis, and acute tonsillitis) have reported variable changes in SWV depending on the stage and

nature of inflammation<sup>26–29</sup>. Further research is required to determine the relationship among inflammation, fibrosis, and pleural stiffness in dogs with BOAS.

Assessment of the arytenoid cartilage using ARFI elastography did not reveal any differences in stiffness between the groups or BOAS grades, diverging from the initial hypothesis of this study, which anticipated lower cartilage stiffness in dogs clinically affected by BOAS, the relationship between airway obstruction and laryngeal collapse<sup>30,31</sup> and the correlation between the degree of obstruction and chondromalacia progression described in BOAS patients<sup>32</sup>. Although this process of laryngeal cartilage degeneration is chronic, it has been described even in 6-month-old animals<sup>32,33</sup>. However, no alterations were identified in this tissue using ARFI elastography in our study.

Arytenoid cartilage stiffness evaluated using ARFI elastography did not differ between brachycephalic and CO or among the BOAS grades. This result contradicts our initial hypothesis that brachycephalic dogs would exhibit reduced cartilage stiffness owing to airway obstruction and laryngeal collapse. Previous studies have linked laryngeal cartilage degeneration to chronic airway obstruction and chondromalacia in brachycephalic dogs and young animals<sup>30–33</sup>. Histological studies have confirmed greater cartilage degeneration in brachycephalic dogs, which contributes to laryngeal collapse under negative airway pressure<sup>34</sup>. However, technical challenges such as rapid breathing, stress, and positional issues may compromise the reliability of our elastography results. Future studies using sedation or anesthesia may improve the accuracy of laryngeal assessments.

Body weight also influenced elastography findings<sup>35,36</sup>. The laryngeal SWV demonstrated a strong positive correlation with body weight, likely due to increased subcutaneous adipose tissue altering wave propagation. Although the BCS did not correlate with laryngeal SWV in this study, this may reflect the limited representation of overweight animals. Further studies with larger populations of obese dogs are necessary to better understand this relationship.

The depth of the tissue evaluation is another critical factor in ARFI elastography. Previous research has demonstrated that the SWV decreases in deeper tissues<sup>22</sup>. Although pleural depth did not correlate with pleural SWV in our study, laryngeal depth was positively correlated with laryngeal SWV, contradicting earlier findings. This discrepancy underscores the need for further investigation of the relationship between tissue depth and SWV across various tissues.

Our study has several limitations. B-mode ultrasound assessments of the pleura are highly operator-dependent, and while ARFI elastography is less influenced by operator variability<sup>12</sup>, inter- and intra-observer analyses were not performed to evaluate ultrasound measurements, which could assess the precision and reproducibility of measurements. For future studies, the implementation of these analyses is recommended to ensure greater robustness of the conclusions regarding the ultrasound measurements. Technical challenges in laryngeal evaluation (e.g., rapid breathing and poor tolerance to handling) may have affected our results. Sedation or anesthesia can mitigate these challenges in future studies. Additionally, our study population did not include older and obese animals, which may have influenced the pleural and laryngeal findings. Finally, histological evaluation of the pleura and laryngeal cartilage was not feasible because of the risks associated with invasive procedures, and laryngoscopy was not performed to confirm or exclude laryngeal collapse.

In conclusion, our findings suggest that inspiratory effort in dogs with BOAS induces secondary pleural changes that are detectable using B-mode ultrasound and elastography. However, no measurable alterations were observed in the arytenoid cartilage. These results reinforce the utility of respiratory ultrasonography for assessing pleural line thickness and rigidity, which correlate with respiratory biomechanics. Further studies incorporating histological evaluations, advanced imaging, and larger and more diverse populations are needed to validate these findings and improve our understanding of tissue-level changes in BOAS.

## Methods

### Ethical aspects

This study adhered to the recommendations of the Brazilian National Council for the Control of Animal Experimentation (CONCEA) and was approved by the Institutional Ethics Committee on the Use of Animals of São Paulo State University (UNESP; protocol No. 3887/21). The owners of the dogs included in this study signed an informed consent form authorizing their animal participation.

### Study design and animals

This prospective observational study was conducted between March and October 2022. The study included 52 brachycephalic dogs (pugs and French bulldogs) from partner breeders and owners, who formed the brachycephalic group. Fifteen beagle dogs from the Unesp Nutrition Laboratory were included in the CO. Inclusion criteria: dogs must belong to the specified breeds, be adults aged 1–8 years, and weigh between 5 and 15 kg. The exclusion criteria were as follows: dogs that underwent surgical procedures to alleviate BOAS signs, those exhibiting clinical signs of non-BOAS systemic diseases at the time of evaluation or in the preceding six months, and those who could not tolerate the proposed evaluations.

### Clinical assessment

All animals underwent a clinical examination to assess their health status and body condition score (BCS) using a 1–9 scale as described previously<sup>37</sup>. After 20 min resting, the BOAS functional assessment was conducted using a 3-min exercise tolerance test, followed by laryngeal auscultation as described and validated by Riggs et al.<sup>38</sup>. This assessment classified dogs into the following categories: Grades 0–I: clinically unaffected by BOAS, exhibiting no or mild respiratory signs with no impact on exercise tolerance; Grades II–III: Clinically affected by BOAS, with moderate to severe respiratory signs requiring surgical intervention. Pre- and post-exercise clinical signs were used for classification, while isolated anatomical changes, such as nostril stenosis and tracheal hypoplasia, were not considered.

## Radiographic examinations

After clinical assessment and BOAS staging, the dogs were taken to an air-conditioned imaging laboratory where they rested for 15 min before radiographic examination. A conventional radiography device (RG150/100gl, Siemens, Munich, Germany) was used to acquire digital images (35 × 43 cm cassette, AGFA-Gevaert N.V., Mortsel, Belgium), later scanned into digital format (CR-30, AGFA-Gevaert N.V.). Three chest radiographic projections—ventrodorsal, right laterolateral, and left laterolateral—were obtained.

## Ultrasound assessment

Following the radiographic examination, the animals were allowed to rest for an additional 15 min. Hair from the left and right chest and ventral cervical areas were clipped to facilitate transcutaneous ultrasonographic examination, and a hydrophilic gel was applied. No sedation was performed during the procedure. A Siemens Acuson S2000 ultrasound device (Munich, Germany) with a 9 MHz linear transducer was used for both B-mode and elastography evaluations.

## Laryngeal B-mode ultrasound

B-mode ultrasonography was performed on the laryngeal cartilage in transverse and longitudinal orientations, following a previously described protocol<sup>39</sup>. The assessments focused on the echotexture, echogenicity, contours, and arytenoid cartilage motility to detect signs of laryngeal collapse. The same experienced evaluator conducted all the examinations to ensure consistency.

## Pleural B-mode ultrasound

The pleural line and lung fields were evaluated using B-mode ultrasound in all the intercostal spaces (right and left hemithorax). The transducer was positioned in both dorsal and transverse approaches, systematically scanning the ventral and dorsal regions to avoid rib artifacts. The Vet Blue protocol<sup>40</sup> was used to sequentially examine four regions of each hemithorax (caudodorsal lung lobe, perihilar, middle, and cranial), as well as the subxiphoid window, totaling nine evaluated regions. Parameters assessed included: changes in the “alligator sign”, discontinuity or absence of A-lines, presence of B-lines, detection of consolidated lung areas with atelectasis. The pleuropulmonary line thickness was measured in all ultrasound windows.

## ARFI elastography

ARFI elastography was performed using the Virtual Touch Tissue Quantification software (Siemens, Germany), which, once activated on the B-mode ultrasound image, creates an elastogram. Homogeneous greenish elastograms indicated high quality, whereas heterogeneous yellowish elastograms indicated low quality, prompting repeat scans. For quantitative analysis in the same elastogram of each tissue, we randomly selected regions of interest (ROIs) to automatically measure the shear wave velocity (SWV, m/s) for the larynx (Laryngeal SWV), five ROIs in standardized longitudinal cuts of the arytenoid cartilages (a pilot study of this project demonstrated that this approach was simpler and improved data consistency) and pleura (Pleural SWV), and three ROIs in each ultrasound window evaluated during B-mode assessment.

## Statistical analysis

Statistical analysis was performed with the help of software R (R, Foundation for Statistical Computing, Vienna, Austria). Initially, Shapiro-Wilk and Bartlett tests were applied to validate if collected variables had normal distribution and variance homoscedasticity. Subsequently, repeated measurements (ROI's and areas) of pleural line thickness, pleural SWV and Laryngeal SWV were compared with each other by the Kruskal-Wallis test, if similarity was found between the different ROIs and regions, a median of pleural line thickness, pleural SWV and Laryngeal SWV was calculated for later evaluations. Subsequently, demographic variables (age, weight and BSC) were compared between the control group (CO) or brachycephalic (BOAS G0, GI, GII and GIII) groups by means of ANOVA, if this was significant, the Tukey post-test was applied, and the data are presented as the mean ± standard deviation (SD). The measurements of pleural line thickness, pleural SWV and Laryngeal SWV were compared between the CO or brachycephalic groups (BOAS G0, GI, GII and GIII) using the Kruskall-Wallis test, if this was significant, the Dunn's post-test was applied, and the data are presented as the median ± interquartile range (IQR). Additionally, discriminative power analysis (CO and BOAS G0 vs. BOAS GI, GII and GIII) was performed through receiver operating characteristic curves (ROC) analysis and calculated the cutoff value (CV), sensitivity and specificity, using the logistic regression model. Additionally, correlation analysis was performed between clinical, and ultrasound studied variables, by Spearman's test. For all tests, the significance was set as  $p < 0.05$ .

## Data availability

The datasets generated and analyzed during this study are available from the corresponding author upon reasonable request.

Received: 1 August 2024; Accepted: 17 March 2025

Published online: 06 June 2025

## References

1. Lindsay, B., Cook, D., Wetzel, J. M., Siess, S. & Moses, P. Brachycephalic airway syndrome: Management of post-operative respiratory complications in 248 dogs. *Aust. Vet. J.* **98**, 173–180 (2020).
2. Ladlow, J., Liu, N. C., Kalmar, L. & Sagan, D. Brachycephalic obstructive airway syndrome. *Vet. Rec.* **182**, 375–378. <https://doi.org/10.1136/vr.k1403> (2018).

3. Mitze, S., Barrs, V. R., Beatty, J. A., Hobi, S. & Bęczkowski, P. M. Brachycephalic obstructive airway syndrome: Much more than a surgical problem. *Vet. Q.* **42**, 213–223. <https://doi.org/10.1080/01652176.2022.2145621> (2022).
4. Hoareau, G. L., Jourdan, G., Mellema, M. & Verwaerde, P. Evaluation of arterial blood gases and arterial blood pressures in brachycephalic dogs. *J. Vet. Intern. Med.* **26**, 897–904 (2012).
5. Troy, L. K. et al. Nocturnal hypoxaemia is associated with adverse outcomes in interstitial lung disease. *Respirology* **24**, 996–1004 (2019).
6. Zhou, B., Yang, X., Zhang, X., Curran, W. J. & Liu, T. Ultrasound elastography for lung disease assessment. *IEEE Trans. Ultrason. Ferroelectr. Freq. Cont.* **67**, 2249–2257 (2020).
7. Friedman, S., Sadot, E., Gut, G., Armoni Domany, K. & Sivan, Y. Laryngeal ultrasound for the diagnosis of laryngomalacia in infants. *Pediatr. Pulmonol.* **53**, 772–777 (2018).
8. Huang, H. et al. The role of laryngeal ultrasound in diagnosis of infant laryngomalacia. *Int. J. Pediatr. Otorhinolaryngol.* **124**, 111–115 (2019).
9. Gómez-López, L. et al. Ultrasound measurement of anatomical parameters of the upper airway in adults. *Rev. Esp. Anestesiol. Reanim.* **65**, 495–503 (2018).
10. You-Ten, K. E., Siddiqui, N., Teoh, W. H. & Kristensen, M. S. Point-of-care ultrasound (POCUS) of the upper airway. *Can. J. Anesth.* **65**, 473–484. <https://doi.org/10.1007/s12630-018-1064-8> (2018).
11. Eom, K. et al. Veterinary science ultrasonographic evaluation of tracheal collapse in dogs. *J. Vet. Sci.* **9**, 401–405 (2008).
12. Gennisson, J. L., Deffieux, T., Fink, M. & Tanter, M. Ultrasound elastography: Principles and techniques. *Diagn. Interv. Imaging* **94**, 487–495 (2013).
13. Constanza, B., Minniti, S., Bucci, A. & Pozzi Mucelli, R. ARFI: From basic principles to clinical applications in diffuse chronic disease—a review. *Insights Imaging* **7**, 735–746 (2016).
14. Manolescu, D., Davidescu, L., Traila, D., Oancea, C. & Tudorache, V. The reliability of lung ultrasound in assessment of idiopathic pulmonary fibrosis. *Clinic. Interv. Aging.* **13**, 437–449. <https://doi.org/10.2147/CIA.S156615> (2018).
15. Oricco, S., Medico, D., Tommasi, I., Bini, R. M. & Rabozzi, R. Lung ultrasound score in dogs and cats: A reliability study. *J. Vet. Intern. Med.* **38**, 336–345 (2024).
16. Kreuter, M. & Mathis, G. Emergency ultrasound of the chest. *Respiration* **87**, 89–97. <https://doi.org/10.1159/000357685> (2014).
17. Almudena, A. O., Alfonso María, L. S., Estefanía, R. G., Blanca, G. H. M. & Simón Pedro, L. L. Pleural line thickness reference values for preterm and term newborns. *Pediatr. Pulmonol.* **55**, 2296–2301 (2020).
18. De Lorenzi, D., Bertoncello, D., Drigo, M. D. & Lorenzi,.. Bronchial abnormalities found in a consecutive series of 40 brachycephalic dogs. *J. Am. Vet. Med. Assoc.* **235**, 835–840 (2009).
19. Hassan, M. et al. Imaging of pleural disease. *Breathe* **20**, 230172. <https://doi.org/10.1183/20734735.0172-2023> (2024).
20. Manson, W. C., Bonz, J. W., Carmody, K., Osborne, M. & Moore, C. L. Identification of sonographic B-lines with linear transducer predicts elevated B-type natriuretic peptide level. *West JEM* **12**, 102–106 (2011).
21. Tasci, O., Hatipoglu, O. N., Cagli, B. & Ermis, V. Sonography of the chest using linear-array versus sector transducers: Correlation with auscultation, chest radiography, and computed tomography. *J. Clin. Ultrasound* **44**, 383–389 (2016).
22. Holdsworth, A., Bradley, K., Birch, S., Browne, W. J. & Barberet, V. Elastography of the normal canine liver, spleen and kidneys. *Vet. Radiol. Ultrasound* **55**, 620–627 (2014).
23. Facin, A. C. et al. Liver and spleen elastography of dogs affected by brachycephalic obstructive airway syndrome and its correlation with clinical biomarkers. *Sci Rep.* **10**, 16156. <https://doi.org/10.1038/s41598-020-73209-7> (2020).
24. Volpicelli, G. et al. Bedside lung ultrasound in the assessment of alveolar-interstitial syndrome. *Am. J. Emerg. Med.* **24**, 689–696 (2006).
25. Zhang, X. et al. An ultrasound surface wave technique for assessing skin and lung diseases. *Ultrasound Med. Biol.* **44**, 321–331 (2018).
26. Sconfienza, L. M. et al. In-vivo axial-strain sonoelastography helps distinguish acutely-inflamed from fibrotic terminal ileum strictures in patients with Crohn's disease: Preliminary results. *Ultrasound Med. Biol.* **42**, 855–863 (2016).
27. Ece, B. & Aydin, S. Can Shear wave elastography help differentiate acute tonsillitis from normal tonsils in pediatric patients: A prospective preliminary study. *Children* **10**, 704. <https://doi.org/10.3390/children10040704> (2023).
28. Yoğurtçuoglu, B. & Damar, Ç. Renal elastography measurements in children with acute glomerulonephritis. *Ultrasonography* **40**, 575–583 (2021).
29. Bob, F. et al. Is there a correlation between kidney shear wave velocity measured with VTQ and histological parameters in patients with chronic glomerulonephritis? A pilot study. *Med. Ultrason.* **20**, 27–31 (2018).
30. Meola, S. D. Brachycephalic airway syndrome. *Top Comp. Anim. Med.* **28**, 91–96 (2013).
31. Torrez, C. V. & Hunt, G. B. Results of surgical correction of abnormalities associated with brachycephalic airway obstruction syndrome in dogs in Australia. *J. Small Anim. Pract.* **47**, 150–154 (2006).
32. Ekenstedt, K. J., Crosse, K. R. & Risselada, M. Canine brachycephaly: Anatomy, pathology, genetics and welfare. *J. Comp. Pathol.* **176**, 109–115. <https://doi.org/10.1016/j.jcpa.2020.02.008> (2020).
33. MacPhail, C. M. Laryngeal disease in dogs and cats: An update. *Vet. Clin. N. Am.* **50**, 295–310. <https://doi.org/10.1016/j.cvsm.2019.11.001> (2020).
34. Tokunaga, S., Ehrhart, E. J. & Monnet, E. Histological and mechanical comparisons of arytenoid cartilage between 4 brachycephalic and 8 non-brachycephalic dogs: A pilot study. *PLoS One* **15**, 1–10 (2020).
35. Taşkin, D. G. et al. Accuracy rate of shear wave elastography in detecting the liver fibrosis in overweight t and obese children with hepatosteatosis. *Turk. Arch. Pediatr.* **58**, 436–441 (2023).
36. Poul, S. S. & Parker, K. J. Fat and fibrosis as confounding cofactors in viscoelastic measurements of the liver. *Phys. Med. Biol.* **66**, 045024. <https://doi.org/10.1088/1361-6560/abd593> (2021).
37. Laflamme, D. Development and validation of a body condition score system for dogs. *Canine Pract.* **22**, 10–15 (1997).
38. Riggs, J., Liu, N. C., Sutton, D. R., Sargan, D. & Ladlow, J. F. Validation of exercise testing and laryngeal auscultation for grading brachycephalic obstructive airway syndrome in pugs, French bulldogs, and English bulldogs by using whole-body barometric plethysmography. *Vet. Surg.* **48**, 488–496 (2019).
39. Bray, J. P., Lipscombe, V. J., White, R. A. S. & Rudorf, H. Ultrasoundographic examination of the pharynx and larynx of the normal dog. *Vet. Radiol. Ultrasound* **39**, 566–571 (1998).
40. Boysen, S. R. & Lisciandro, G. R. The use of ultrasound for dogs and cats in the emergency room AFAST and TFAST. *Vet. Clin. North Am. Small Anim. Pract.* **43**, 773–797. <https://doi.org/10.1016/j.cvsm.2013.03.011> (2013).

## Acknowledgements

The authors thank the São Paulo Research Foundation (FAPESP/CAPES) (grant numbers 2022/07366-0 and 2021/04147-2) and the National Council for Scientific and Technological Development (CNPq) for funding this study (productivity scholarship 305182/2020-0). Gratitude was also extended to the owners and breeders of the participating dogs.

## Author contributions

A.R., R.A.R.U, M.A.R.F, and P.C.M.: conception and design; A.R., A.C.F., B.B.L., B.G., L.P.A., I.A.F. and M.A.R.F: acquisition of Data; A.R., R.A.R.U and M.A.R.F.: analysis and interpretation of data; A.R., A.C.F., R.A.R.U., M.A.R.F. and P.C.M.: drafting the article; all authors approved the final version of the completed article. All authors approved the final version of the completed article.

## Declarations

### Competing interests

The authors declare no competing interests.

### Additional information

**Correspondence** and requests for materials should be addressed to M.A.R.F.

**Reprints and permissions information** is available at [www.nature.com/reprints](http://www.nature.com/reprints).

**Publisher's note** Springer Nature remains neutral with regard to jurisdictional claims in published maps and institutional affiliations.

**Open Access** This article is licensed under a Creative Commons Attribution-NonCommercial-NoDerivatives 4.0 International License, which permits any non-commercial use, sharing, distribution and reproduction in any medium or format, as long as you give appropriate credit to the original author(s) and the source, provide a link to the Creative Commons licence, and indicate if you modified the licensed material. You do not have permission under this licence to share adapted material derived from this article or parts of it. The images or other third party material in this article are included in the article's Creative Commons licence, unless indicated otherwise in a credit line to the material. If material is not included in the article's Creative Commons licence and your intended use is not permitted by statutory regulation or exceeds the permitted use, you will need to obtain permission directly from the copyright holder. To view a copy of this licence, visit <http://creativecommons.org/licenses/by-nc-nd/4.0/>.

© The Author(s) 2025